



ISSN: 0067-2904

GIF: 0.851

## A new mode for an on-line determination of Pyrocatechol, Resorcinol, and Pyrogallol in pure commercial samples using CFIA with homemade Ayah 3S<sub>BGR</sub>x3- 3D solar cell microphotometer analyzer.

Nagam S. TurkieAl-Awadie \*, Malik H. AlalooshAlamri

Department of chemistry, College of science, University of Baghdad, Baghdad,Iraq.

### Abstract:

A new, simple, accurate, fast and sensitive spectrophotometric method has been developed for the analysis of Pyrocatechol, Resorcinol, and pyrogallol in pure commercial samples by continuous flow injection analysis. The method was based on the oxidation of the organic compounds with Ce(IV)sulfate in acidic medium to form a brown colored species which determined using homemade Ayah 3S<sub>BGR</sub> x3-3D solar cell flow injection microphotometer. Optimum conditions were obtained using a high intensity green light emitted diode as an irradiation source for Pyrocatechol, Resorcinol, while blue light emitted diode as an irradiation source for pyrogallol. The linear dynamic range for the instrument response versus Pyrocatechol, Resorcinol, and pyrogallol concentrations were 5-40 mmol.L<sup>-1</sup> while the L.O.D was of 36.63, 17.17, and 41.61 ng / sample respectively. The correlation coefficient (r) was 0.9952, 0.9970, and 0.9960 while percentage linearity (r<sup>2</sup>%) was 99.05%, 99.41% and 99.22% for Pyrocatechol, Resorcinol, and pyrogallol respectively. RSD% for the repeatability (n=8,7, and 8) was 1.4%, 0.63%, 1.78% for the determination of Pyrocatechol, Resorcinol, and pyrogallol, respectively at concentration of 30 mmol.L<sup>-1</sup>. The method was applied successfully for the determination of three organic compounds in pure commercial samples. A comparison was made between the newly developed method and the classical method (UV-Vis spectrophotometry) at wave length 492, 481, and 438 nm for Pyrocatechol, Resorcinol and pyrogallol respectively of analysis using the standard additions method via the use of paired t-test. It was noticed that there is no significant difference between two different methods for analysis three different organic compounds; in addition to no significant difference in the contribution of the Pyrocatechol, Resorcinol and pyrogallol to the oxidant reaction path, at 95% confidence level.

**Key words:** Pyrocatechol, Resorcinol, Pyrogallol, Flow injection analysis, Spectrophotometry.

نمط جديد للتقدير الأني للبايروكتكول، ريزورسينول و البايروكالكول في نماذج تجارية نقية باستخدام

التحليل بالحقن الجرياني المستمر عن طريق استخدام محلل طيفي مايكروبي مصنع محليا Ayah

3S<sub>BGR</sub> x3-3D solar cell.

نغم شاكر تركي العوادي \* ، مالك حسين العلوش العامري

قسم الكيمياء، كلية العلوم، جامعة بغداد ، بغداد ، العراق .

### الخلاصة:

طورت طريقة طيفية جديدة، بسيطة، سريعة، مضبوطة، وحساسة لتحليل البايروكتكول، الريزورسينول، والبايروكالكول في نماذج تجارية نقية باستخدام التحليل بالحقن الجرياني المستمر. استندت الطريقة على أكسدة المركبات العضوية بكبريتات السيريوم (IV) في الوسط الحامضي لتكوين اصناف ملونة بنية والتي قدرت

بأستخدام مطياف مايكروبيالاحقن الجرياني المستمر مع Ayah 3S<sub>BGR</sub> x3-3D solar cell المصنع محليا. تم دراسة الظروف الفضلى التي تم التوصل اليها بأستخدام ثنائي الوصلة باعث للضوء الاخضر وبشدة عالية كمصدر لتشعيعالبايروكتكول والريزورسينول، بينماتثاني الوصلة باعث للضوء الازرق وبشدة عالية كمصدر لتشعيع البايروكالول . المدى الخطي الفعال لعلاقة تغير الاستجابة الألية مع التركيز ٥ - ٤٠ مللي مول.لتر<sup>-١</sup> بينما حدود الكشف 36.63, 17.17, ٤١.٦١, ١٧.١٧ / ناغم / انموذج. وان معامل الارتباط (r) ٠.٩٩٥٢, ٠.٩٩٧٠, و ٠.٩٩٦٠. بينما نسبة الخطية R<sup>2</sup> = ٩٩.٠٥, ٩٩.٤١, و ٩٩.٢٢. الانحراف القياسي النسبي المؤي (RSD%) للتكرارية (n= 8,7,8) ١.٤, ٠.٦٣, ١.٧٨ % لمحلول البايروكتكول، الريزورسينول، والبايروكالول بتركيز ٣٠ مللي مول لتر<sup>-١</sup> للبايروكتكول، الريزورسينول والبايروكالول طبقت الطريقة بنجاح لتقدير المركبات العضوية الثلاثة في نماذج تجارية نقيه. اجريت مقارنة بين الطريقة المطورة والطريقة التقليدية (مطيافية UV-Vis) عند طول موجي ٤٣٨، ٤٨١، و ٤٩٢ نانو متر للتليل باستخدام منحنى الاضافات القياس من خلال استخدام اختبار t-المزدوج. لوحظ انه لا يوجد فرق جوهري بين الطريقتين لتليل المركبات العضوية الثلاثة بالاضافة الى عدم الاختلاف في مساهمة كل من البايروكتكول ، الريزورسينول و البايروكالول على مسار تفاعل الاكسدة عند مستوى قنعة ٩٥%.

## Introduction:

Aromatic hydroxyl phenols are common chemicals used in industries as well as in clinical and biochemical applications [1]. Polyphenols are common constituents of the human diet, present in most foods and beverages of plant origin. Polyphenol are considered to contribute to the prevention of various degenerative diseases, including cardiovascular diseases [2]. Polyphenol compounds are highly abundant in nature, since they are the essential raw materials and byproducts of vast chemical industries. Some of these compounds are extremely toxic and resistant to biotic and abiotic degradation [3,4]. Polyphenols and phenolic compounds are found mostly in plants and effluents of industries, such as coal conversion, paper and pulp manufacturing, wood preservation, metal casting, polyphenol compounds are considered to be hazardous pollutants [5]. Furthermore, the breakdown products of polyphenol may be more harmful when phenol is incompletely degraded by physical and chemical methods or by natural oxidation. Therefore, the complete removal of these substances from industrial and domestic water bodies is of great importance for conservation of native biodiversity [6]. Catechol (Cat, figure-1A) , 1,2-dihydroxybenzene, 1,2-benediol, pyrocatechol, this chemical was first obtained by dry distillation of catechin by Reinsch in 1839. It is widely distributed in nature and found in plants (onion, eucalyptus, crudebeetsugar), coal and tobacco smoke. It is a colourless crystalline solid (monoclinic crystals) and discolours when in contact with air and light. It readily dissolves in water and hydrophobic organic solvents (ethanol and acetone) [7]. Cat is used in a variety of applications. It is used as a reagent for photography, dyeing fur, rubber and plastic production, pesticides and in pharmaceutical industries[8,9]. Catechols can undergo a variety of chemical reactions, such as complex formation and redox chemistry of catechols. In presence of heavy metals such as iron or copper, stable complexes can be formed [10 -12]. Substituted catechols, especially chlorinated and methylated catechols, are by-products in pulp and oil mills [13,14]. Resorcinol (Res, figure-1B) is the 1,3-isomer of benzenediol [15]. Res is a dihydric phenol and exhibits the typical reactivity of a phenol [16]. Res is a white to off-white needle-like crystals, flakes or powder. When exposed to light and air resorcinol crystals acquire a pale red [17,18]. Res is a monoaromatic compound with two hydroxyl group in meta position to each other. It occurs naturally in fossil fuels, in heartwood of Artocarpus and Morus (Moraceae) species [19]. And in exudates of Nupharlutea [20]. Res readily soluble in water, alcohol, and ether, but insoluble in chloroform and carbon disulfide [21]. The resorcinol moiety has been found in a wide variety of natural products. In particular, the plant phenolics, of which resorcinol ring-containing constituents are a part, are ubiquitous in nature and are well documented[22]. Res used externally, it is an antiseptic and disinfectant, and is used 5 to 10% in ointments in the treatment of chronic skin diseases such as psoriasis, hidradenitissuppurativa, andeczema [23]. Resorcinol is a monomeric by-product of the reduction, oxidation, and microbial degradation of humic substances [24,25].

Pyrogallol (Pyr, figure- 1C) is an organic compound: 1,2,3-benzenetriol, 1,2,3-trihydroxybenzene .It is a white solid crystals; grayish on exposure to air and light, although because of its sensitivity toward oxygen, samples are typically brownish. It is one of three isomeric benzenetriols [26,27]. Pyr (1,2,3-trihydroxy benzene), a polyphenol has been exploited in a variety of industrial sector, for example, as a developer in photography, to make colloidal solutions of metals, as a mordant for wool, for staining leather, in process engraving, in the manufacture of various dyes, and in the dyeing of fur, hair. In analytical chemistry it is used as a reagent for antimony and bismuth. [28,29]. Pyr was the first synthetic organic dye used on human hair, Pyr is used as a modifier in oxidation dyes . Pyr is present in 42 hair dyes and colors . And the Pyr concentration in the dyes and colors typically ranges from 0.25 to 0.38% by weight [30,31] . Pyr is the end product in ruminal bacteria like *Selenomonas* ,and *Streptococcus*. [32,33].

Methods have been reported for determination of Cat, Res, and Pyr, , GC- FID [34,35]. HPLC [36- 38] .voltammetry [39-43]. Spectrophotometry [44-46].

The proposed method based on the oxidation of Cat, or Res, or Pyr byCe (IV) sulfate in acidic medium. The oxidation product yields as a brown color which measured by Ayah 3S<sub>BGRX3</sub>-3D solar cell CFIA microphotometer (homemade) [47] at 492,481, 438 nm for Cat, Res, and Pyr respectively. The procedure is simple, rapid and is proposed for the control analysis as an alternative analytical procedure.

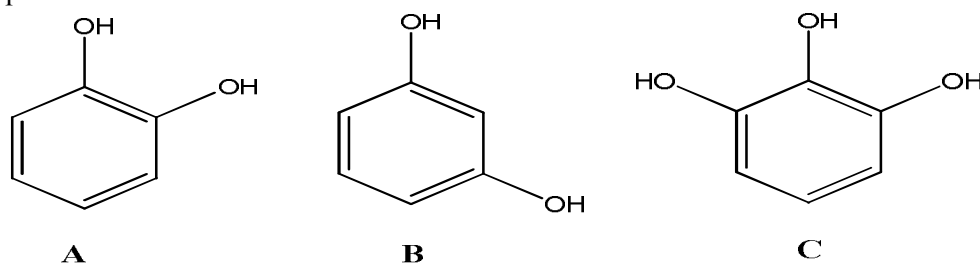


**Figure 1-** Chemical structure of ; A: Cat, B: Res, C: Pyr.

## Experimental:

### Chemicals:

All chemicals were used of analytical-reagent grade while distilled water was used to prepare the solutions. A standard solution 0.5 M of Cat ( $C_6H_4(OH)_2$  M.Wt. 110.1  $g \cdot mol^{-1}$ , BDH) was prepared by dissolving 13.7625 g in 250 ml of distilled water. A standard solution 0.5 M of Res ( $C_6H_4(OH)_2$  M.Wt. 110.1  $g \cdot mol^{-1}$ , BDH) was prepared by dissolving 13.7625 g in 250 ml of distilled water. A standard solution 0.5 M of Pyr ( $C_6H_4(OH)_3$  M.Wt. 126.11  $g \cdot mol^{-1}$ , BDH) was prepared by dissolving 15.76372 g in 250 ml of distilled water. A stock solution 0.1M of Ce(IV) sulfate (  $Ce(SO_4)_2$  M.Wt 332.298  $g \cdot mol^{-1}$  , Hopkin& Williams LTD) was prepared by dissolving 16.614 g in 500 ml of sulphuric acid 1M, ( $H_2SO_4$ , M.Wt 98  $g \cdot mol^{-1}$ , 18 M, sp.g 1.84 $g \cdot ml^{-1}$ , percentage 96%, BDH) (standardized against 1M  $Na_2CO_3$  solution ) was prepared by diluting 27.7ml of the sulphuric acid in distilled water to final volume 500ml by using volumetric flask 500 mL. Hydrochloric acid solution 1M (35%, 1.19  $g \cdot ml^{-1}$ , BDH) were prepared by pipetting 21 mL of concentrated hydrochloric acid and completed of the volume with distilled water in 250 mL volumetric flask. Nitric acid solution 1M (70%, 1.42  $g \cdot ml^{-1}$ , BDH) was prepared by pipetting 16 mL of concentrated nitric acid and completed the volume with distilled water into 250 mL- volumetric flask. All acids were standardized with  $Na_2CO_3$  solution. A stock solution 1M of sodium carbonate ( $Na_2CO_3$ , 106  $g \cdot mol^{-1}$  , BDH) was prepared by dissolving 26.50 g in 250 mL.

Sample preparation: pyrocatechol – Readeldehean, resorcinol- Randwin, and pyrogallol- Readeldehean, were weighted: 5.505 g , 5.505, and 6.3055 g respectively, which dissolved in 100 ml of distilled water to obtained concentration equivalent to 500  $mmol \cdot l^{-1}$  for each sample.

### Apparatus and manifold:

The flow system used for the determination of Cat, Res, and Pyr shown schematically in figure- 2, peristaltic pump four channels variable speed (Ismatec, Switzerland). Valve 6 – port medium pressure injection valve ( I D E X corporation, USA) with sample loop (1 mm i.d., Teflon , variable

length ). The instrument response was measured by Ayah 3S<sub>BGR</sub> x 3 – 3 D solar cell continuous flow injection analysis microphotometer ( homemade ) [47 ] by using three super bright blue470 nm , green 525nm and red 635 nm light emitted diode (LED ) as a source , three solar cell as a detector. The output signals were recorded by potentiometric recorder (Siemens, Germany, 1- 500 Volt, 1-500 mV). Peak height was measured for each signal. UV-Vis Spectrophotometer digital double beam type (UV- Vis spectrophotometer: UV-1800, shimadzu, and spectronic 20D +, Japan) were also used to scan the spectrum of colored species using 1cm glass cell.

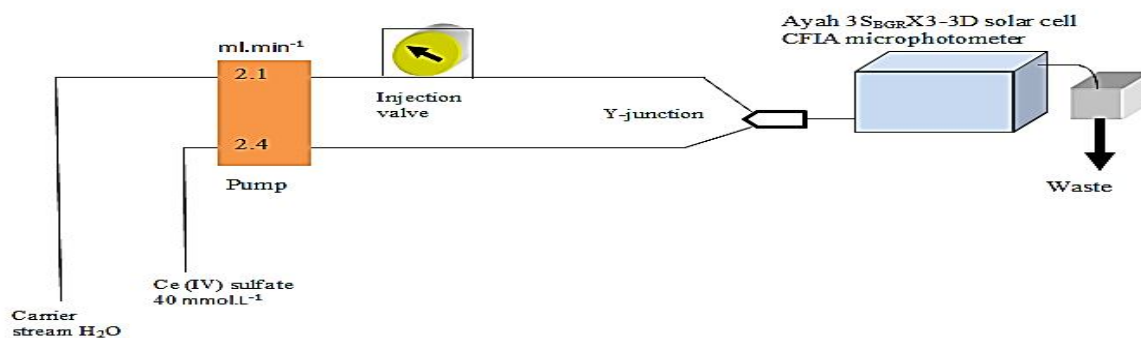
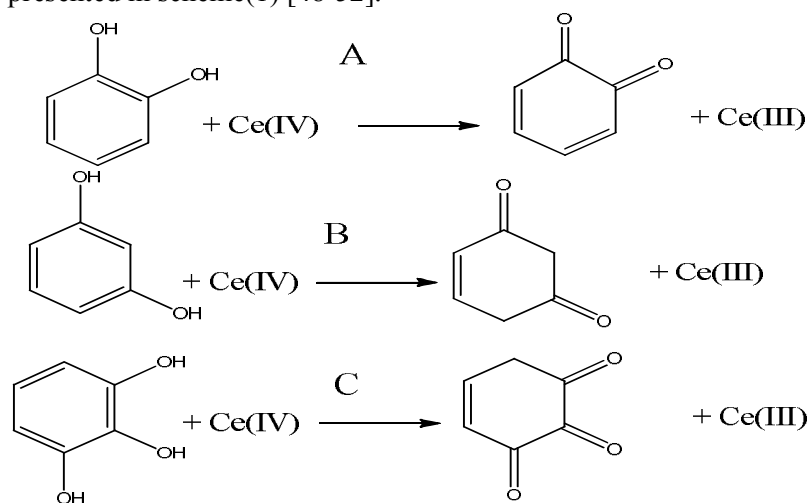


**Figure 2**-schematic diagram of Continuous Flow Injection Analysis system with Ayah 3S<sub>BGR</sub> X

3 - 3D solar cell CFIA microphotometer, for determination of Cat, Res, and Pyr.

### Methodology:

The whole reaction manifold system of Cat, Res, and Pyr determination by direct oxidation via Ce(IV) sulfate in acidic medium to form colored species was shown in Figure- 2 . The manifold system is composed from two lines: The first line supplied distilled water as a carrier stream at 2.1 ml.min<sup>-1</sup> which leads to the injection valve for carrying samples with 165, 156, and 165 μ L for Cat, Res, and Pyr respectively sample volume (loop length: 21.0, 19.82, and 21.0 cm, with 1mm I.D. ) , the second line supplied Ce(IV) sulfate 40 mmol.L<sup>-1</sup> in acidic medium (500 mmol.L<sup>-1</sup> of H<sub>2</sub>SO<sub>4</sub> ) at 2.4 ml.min<sup>-1</sup> . Both of lines meet at junction (Y- junction) with an outlet for reactants product from brown colored species which passes through Ayah 3S<sub>BGR</sub> x3- 3D solar cell CFIA microphotometer. The variation of response was monitored using green light emitted diode LED (525 nm) for determination of Cat, and Res, while blue light emitted diode LED (470 nm) for determination of Pyr, throughout the reaction to obtain transducer energy response in mV versus time. Each solution was assayed triplicate. A proposed mechanism for oxidation of Cat, Res, and Pyr by Ce(IV)sulfate in acidic medium is presented in scheme(1) [48-52].



**Schematic 1**- proposed mechanism of reaction between: A- Cat, B- Res, C- Pyr and Ce(IV) sulfate in acidic medium.

**Results and discussion:**

**Scanning of spectrum for org. comp. – Ce(IV) sulfate – H<sub>3</sub>O<sup>+</sup> :**

A scanning between 200-600 nm was carried out to obtain  $\lambda_{max}$  for colored product (brown) by oxidation of Cat, Res, and Pyr (5 mmol.L<sup>-1</sup>) with Ce(IV)sulfate (12 mmol.L<sup>-1</sup>) in acidic medium (H<sub>2</sub>SO<sub>4</sub>, 500 mmol.L<sup>-1</sup>). It can be seen clearly that a maximum absorbance at 492, 481, and 438 nm for Cat, Res, and Pyr respectively against reagent blank (Ce(IV) sulfate), as shown in figure- 3A.

Second spectroscopic study for colored species (brown) was monitoring by a homemade Ayah 3S<sub>BGR</sub>X3-3D solar cell CFIA microphotometer at three different super bright light diode (LED) as a source including blue 470nm, green 525 nm, and red 635 nm, selected conditions were used, two lines system (figure- 2 ), 165  $\mu$ L as a sample volume of Cat, Res, and Pyr with concentrations 20, 50, and 50 mmol.L<sup>-1</sup> respectively which injected into the carrier stream (H<sub>2</sub>O) at 2.1 ml.min<sup>-1</sup>, while the Ce(IV) sulfate 50 mmol.L<sup>-1</sup> at 2.4 ml.min<sup>-1</sup> (second line) meet with Cat, Res, and Pyr at Y- junction point in later stage of reaction. A maximum response measured in mV (expressed as transducer energy response) was obtained using high intensity super bright green light emitted diode (LED) for Cat, and Res, while super bright blue light emitted diode (LED) for Pyr. Figure- 3B indicate the profile of the response and intensity. Therefore, the green light emitted diode (LED) was used as a source for determination Cat, and Res, while blue light emitted diode (LED) was used as a source for determination Pyr.

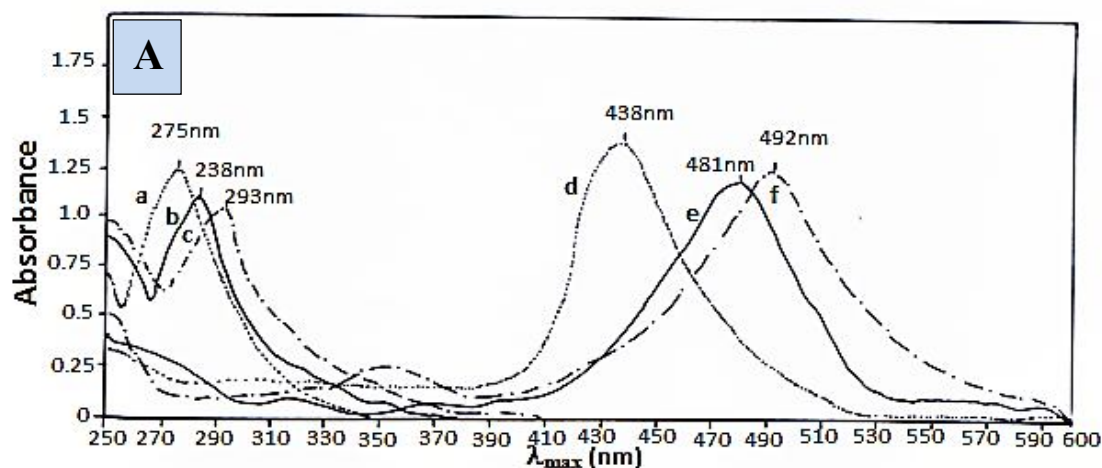


**Figure 3-(A):** Absorbance spectra for: a: Cat, b: Res, and c: Pyr, against the blank (H<sub>2</sub>O), d: Pyr, e: Res, and f: Cat against the blank (Ce(IV)sulfate).

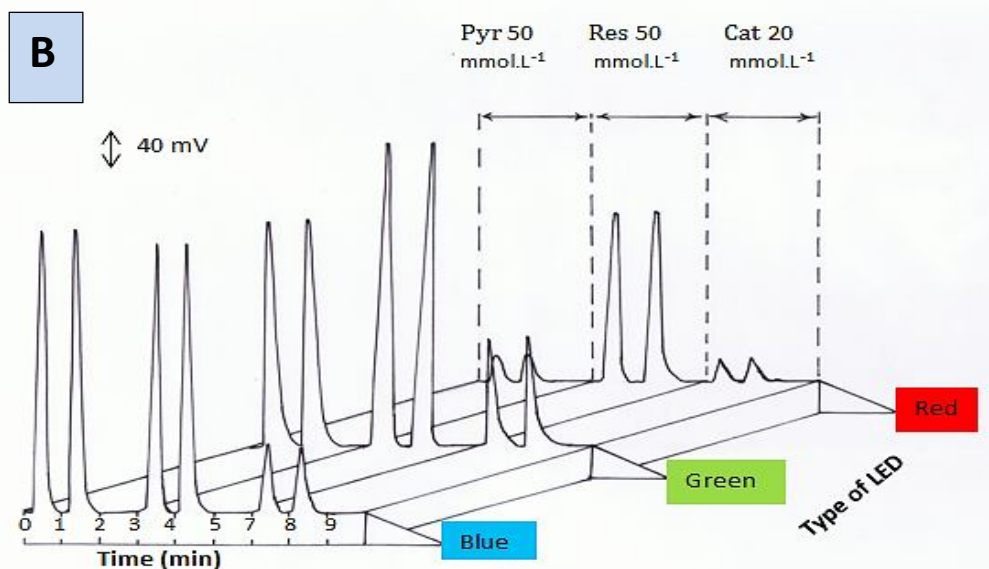


**Figure 3-(B):** A maximum responses profile (mV) versus differences light emitted diode using Ayah 3S<sub>BGR</sub> x 3 – 3D solar cell CFIA microphotometer for Cat(20mmol.l<sup>-1</sup>), Res and, Pyr (50 mmol.L<sup>-1</sup>) –

Ce(IV)sulfate (50 mmol.L<sup>-1</sup>) – H<sub>3</sub>O<sup>+</sup> system, with 165 μL as a sample volume, flow rate 2.1, and 2.4 ml.min<sup>-1</sup> for the carrier stream and reagent (Ce(IV)sulfate) respectively.

### Optimum conditions for oxidation of Cip with Ce (IV) Sulfate in acidic medium.

#### Chemical variables:

#### Effect of Ce(IV) sulfate concentration:

The effect of varying concentration of Ce(IV) sulfate was examined, using a series of solutions ranged 20 – 60 mmol.L<sup>-1</sup> which diluted by 500 mmol.L<sup>-1</sup> of H<sub>2</sub>SO<sub>4</sub>, at 20 mmol.L<sup>-1</sup> of Cat, Res, and Pyr, 165 μL as a sample volume , while two lines manifold system was used at 2.1, and 2.4 ml.min<sup>-1</sup> for the carrier stream (H<sub>2</sub>O) and Ce(IV) sulfate respectively. The obtained results were tabulated in Table1, which Summarizes the average of three successive readings with relative standard deviation and confidence interval of the average response at 95% confidence ( $\alpha = 0.05$ ). Figure- 4 shows the plot of the results as it obtained from Ayah 3S<sub>BGR</sub> x3 -3D solar cell CFIA microphotometer. It was noticed that an increase in the response of the colored species with increasing Ce (IV) Sulfate concentration up to 40 mmol.L<sup>-1</sup> more than 40mmol.L<sup>-1</sup> led to broadening in peak maxima and increase the peak base width ( $\Delta t_b$ ). It is probable that it could be due to the restriction of the passage of incident light due to the accumulation of precipitate in front of the detector which in turn off act on the attenuation of incident light therefore , 40 mmol.L<sup>-1</sup> was chosen as optimum concentration of Ce(IV) sulfate in next studies.

**Table 1-** Variation of Ce (IV) sulfate concentration on the transducer energy response of org. comp – Ce(IV)-H<sub>3</sub>O<sup>+</sup> system .

Type of analyte	[Ce(IV) sulfate] mmol.L <sup>-1</sup>	Average transducer energy response expressed as peak height n=3, $\bar{y}_i$ (mV)	RSD%	Confidence interval of the average response $\bar{y}_i \pm t_{0.05/2, n-1} \sigma_{n-1} / \sqrt{n}$
Cat	20	163	0.6	163 ± 2.49
	30	178	1.12	178 ± 4.97
	40	186	1.0	186 ± 2.86
	50	161.33	0.7	161.33 ± 2.86
	60	130	1.5	130 ± 4.97
Res	20	122	1.6	122 ± 4.97
	30	161	1.42	161 ± 5.71
	40	200	0	200 ± 0
	50	228	1.75	228 ± 9.94
	60	252	1.59	252 ± 9.94
Pyr	20	108.33	1.85	108.33 ± 4.97
	30	129.33	1.78	129.33 ± 5.71
	40	132	1.5	132 ± 4.97
	50	91.33	1.25	91.33 ± 2.85
	60	86	1.3	86 ± 2.85

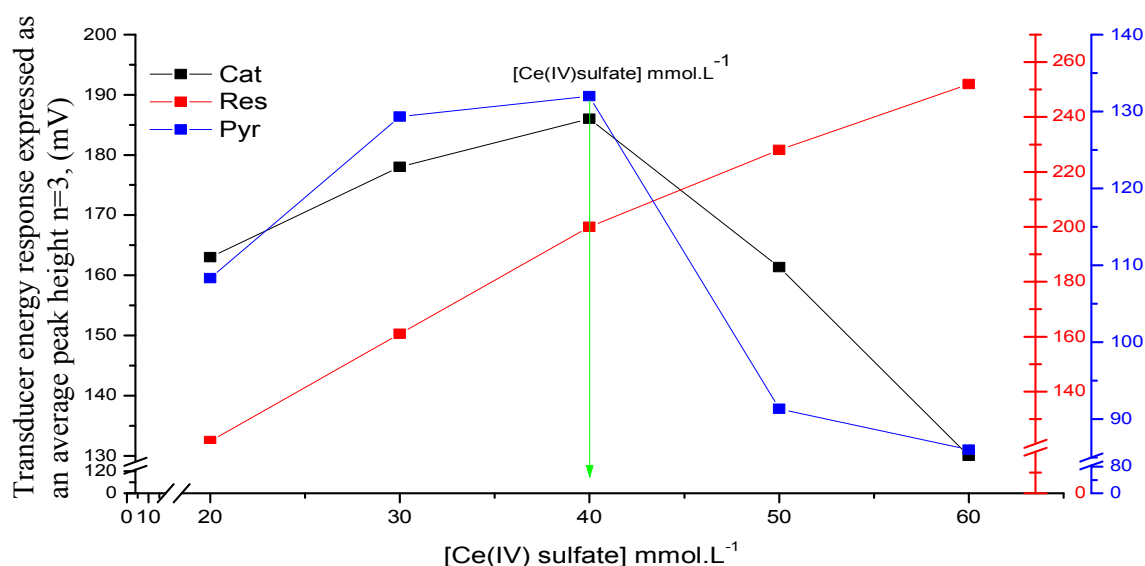


Figure4-Variation of [Ce(IV) sulfate] on transducer energy response (mV).

#### Effect of acidic medium as a carrier stream:

The reaction of Cat, Res, and Pyr with Ce(IV) sulfate can be conducted in acidic medium; therefore different acids were used ( H<sub>2</sub>SO<sub>4</sub>, HCl, HNO<sub>3</sub>, at 50 mmol.L<sup>-1</sup>) in addition to H<sub>2</sub>O as a carrier stream at 2.1 ml.min<sup>-1</sup>, the optimum concentration of Ce(IV) sulfate 40 mmol.L<sup>-1</sup> ( in 500 mmol.L<sup>-1</sup> of H<sub>2</sub>SO<sub>4</sub>) at 2.4 ml.min<sup>-1</sup>, 20 mmol.L<sup>-1</sup> of Cat, Res and Pyr with 165μL sample volume were used. Table 2 shows the obtained results, while figure-5 shows the plot and response profile, it can be seen that the effect of different acids was not very crucial on the decrease of the response heights (figure- 5B) which might be attributed to dissociation of some of the colored species, therefore, distilled water was chosen as optimum carrier stream, which gave suitable sensitivity and response profile.

Table 2- Variation acidic medium as a carrier stream on the transducer energyresponse of org. comp – Ce(IV)-H<sub>3</sub>O<sup>+</sup> system.

Type of analyte	Type of acid	Average transducer energy response expressed as peak height n=3, $\bar{y}_i$ (mV)	RSD%	Confidence interval of the average response $\bar{y}_i \pm t_{0.05/2, n-1} \sigma_{n-1} / \sqrt{n}$
Cat	H <sub>2</sub> O	161.33	0.71	161.33 ± 2.85
	H <sub>2</sub> SO <sub>4</sub>	155.33	1.28	155.33 ± 4.97
	HCl	160	0	160 ± 0
	HNO <sub>3</sub>	160	0	160 ± 0
Res	H <sub>2</sub> O	201.67	1.13	200.67 ± 5.71
	H <sub>2</sub> SO <sub>4</sub>	180	0	180 ± 0
	HCl	187.33	2.22	187.33 ± 10.34
	HNO <sub>3</sub>	172	0	172 ± 0
Pyr	H <sub>2</sub> O	122.67	1.88	122.67 ± 5.71
	H <sub>2</sub> SO <sub>4</sub>	101.33	2.27	101.33 ± 5.71
	HCl	121.33	2.0	121.33 ± 5.571
	HNO <sub>3</sub>	118.33	2.75	118.33 ± 5.16

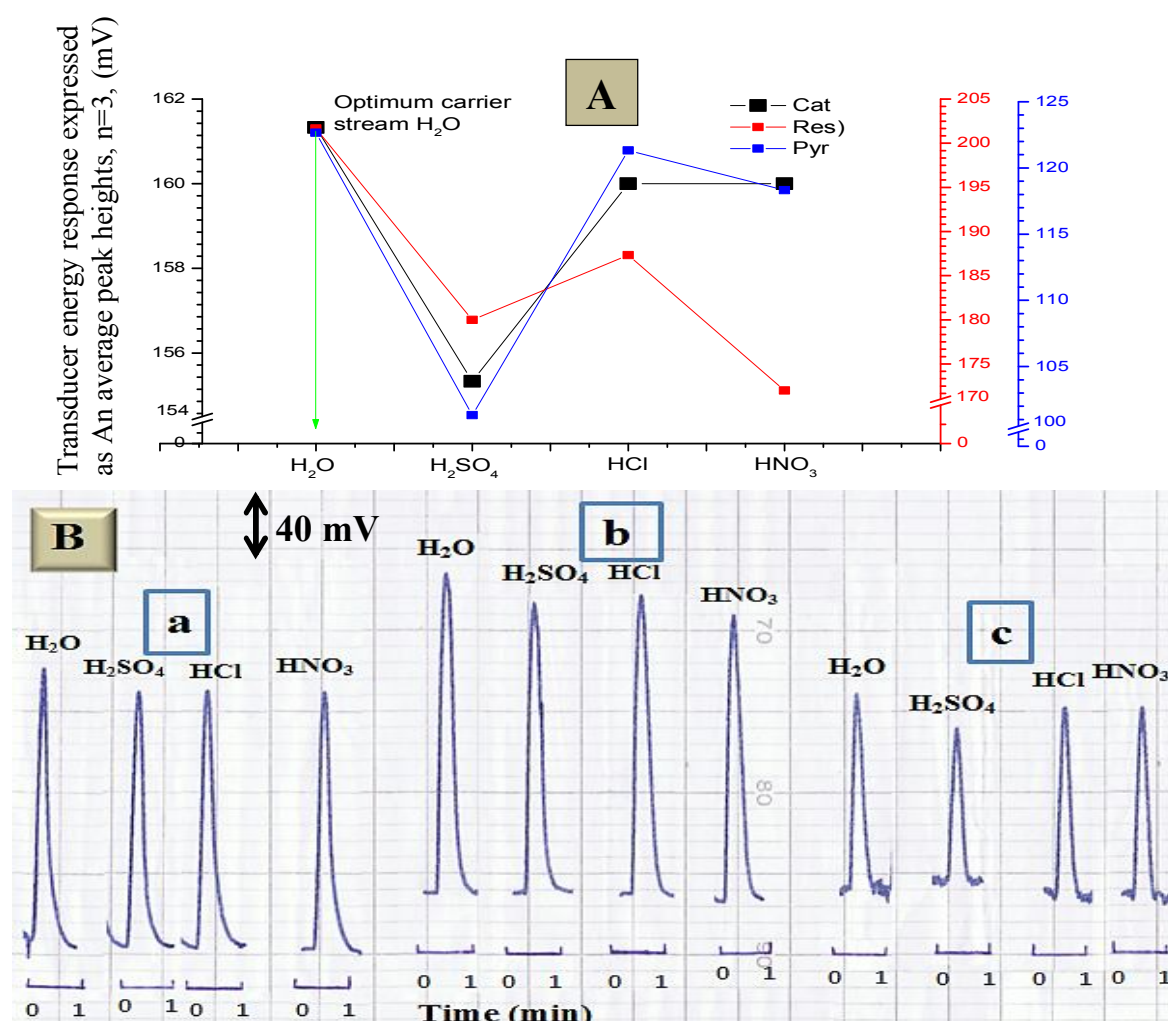


**Figure 5-** Variation type of acidic medium as a carrier stream on: A: Transducer energy response (mV), B: response profile using Ayah 3S<sub>BGR</sub>X 3-3D solar cell CFIA, for determination of, a: Cat, b: Res, and c: Pyr.

**Physical variables:**

**Flow rate:**

Flow rate was ranged 0.4-2.4, and 0.4-2.8 ml.min<sup>-1</sup> for the carrier stream and the reagent (Ce(IV) sulfate) respectively. The flow rate of Cat, Res, and Pyr determination was investigated to conduct the optimize of preferred flow rate. The optimum concentration 40 mmol.L<sup>-1</sup> of Ce(IV) sulfate, and using 30 mmol.L<sup>-1</sup> of Cat, Res, and Pyr with 165 μL as a sample volume, while distilled water was used as a carrier stream. The obtained results were tabulated in Table 3, while figure- 6 shows the plot, and response profile. It was noticed that at low flow rate there were an increase in peak base width, with decrease peak height, and broadening at the peak maxima, which might be due to the dispersion and dilution leading to an irregular response profile (figure- 6B). But at high flow rate influence (up to pump speed 30) led to an increase in peak height, decrease the peak base width, and decrease time that required for arrive the colored species to the measuring flow cell. As compromise between sensitivity, peak shape, and consumption of the chemicals. A 2.1, and 2.4 ml.min<sup>-1</sup> were chosen as optimum flow rate for the carrier stream and Ce(IV) sulfate respectively.

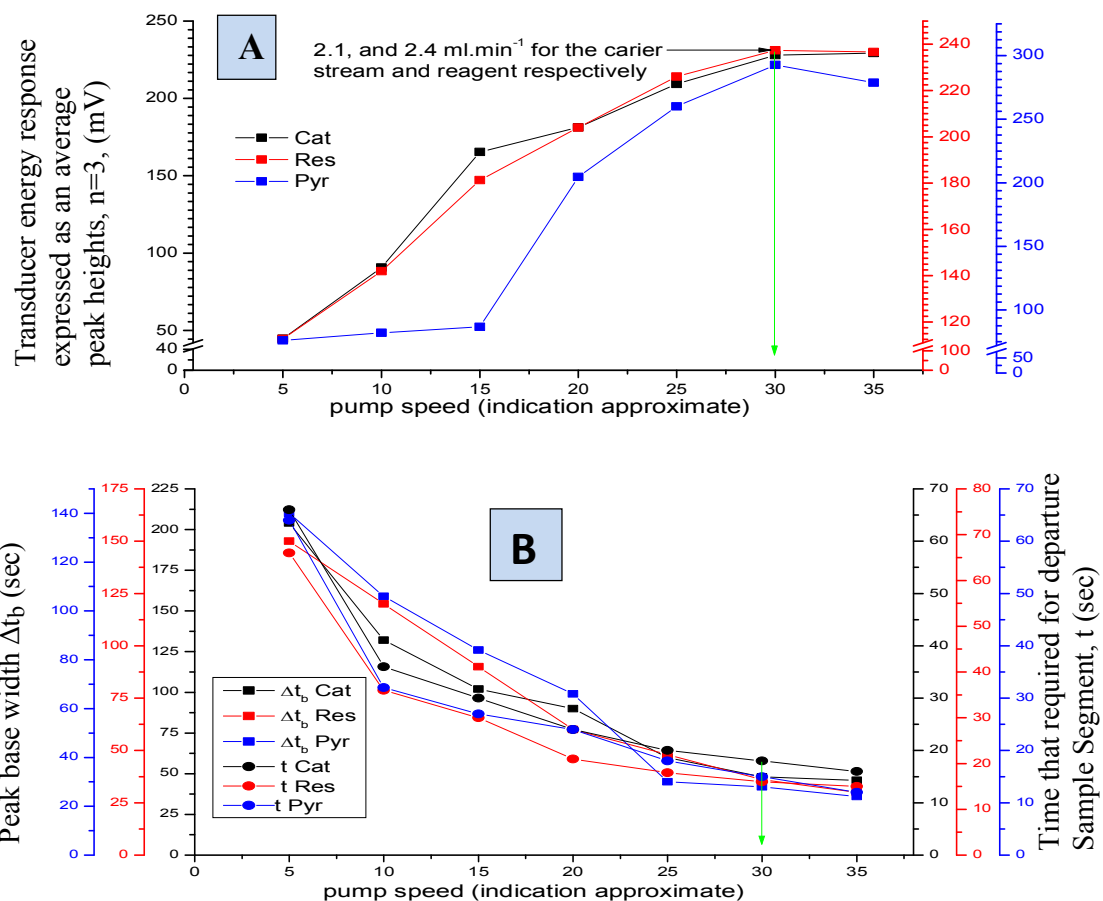


**Table 3-** Variation of flow rate (ml.min<sup>-1</sup>) on the transducer energy response (mV).

Type of Analyte	Pump speed indication approximate	Flow rate (ml.min <sup>-1</sup> )		Average transducer energy response expressed as peak height n=3, $\bar{y}_i$ (mV)	RSD%	Confidence interval of the average response $\bar{y}_i \pm t_{0.05/2, n-1} \sigma_{n-1} / \sqrt{n}$	$\Delta t_b$ sec	t sec
		Carrier stream	Ce(IV) sulfate line					
Cat	5	0.4	0.4	44.67	1.11	44.67 ± 1.41	204	66
	10	0.7	0.7	90.67	1.27	90.67 ± 2.85	132	36
	15	1.1	1.2	165.33	1.2	165.33 ± 4.97	102	30
	20	1.4	1.6	181.33	1.1	181.33 ± 4.97	90	24
	25	1.8	2.0	209.33	1.67	209.33 ± 8.72	60	20
	30	2.1	2.4	228	0	228 ± 0	48	18
	35	2.4	2.8	229.33	1.0	229.33 ± 5.71	46	16
Res	5	0.4	0.4	112.67	1.02	112.67 ± 2.85	150	66
	10	0.7	0.7	142	1.4	142 ± 4.97	120	36
	15	1.1	1.2	181.33	1.26	181.33 ± 5.71	90	30
	20	1.4	1.6	204	0.98	204 ± 4.97	60	21
	25	1.8	2.0	226	0.88	226 ± 4.997	48	18
	30	2.1	2.4	237.33	0.48	237.33 ± 2.85	36	16
	35	2.4	2.8	236.67	0.97	236.67 ± 5.71	30	15
Pyr	5	0.4	0.4	76	1.5	76 ± 2.85	140	64
	10	0.7	0.7	82	1.2	82 ± 2.48	106	32
	15	1.1	1.2	86.67	1.15	86.67 ± 2.48	84	27
	20	1.4	1.6	204.67	0.97	204.67 ± 4.97	66	24
	25	1.8	2.0	260	0	260 ± 0	30	18
	30	2.1	2.4	292.67	0.78	292.67 ± 5.71	28	15
	35	2.4	2.8	278.67	0.82	278.67 ± 5.71	24	12

$\Delta t_b$  (sec): peak base width .

t (sec) : time for the departure of sample segment from injection valve reaching to the measuring flow cell.



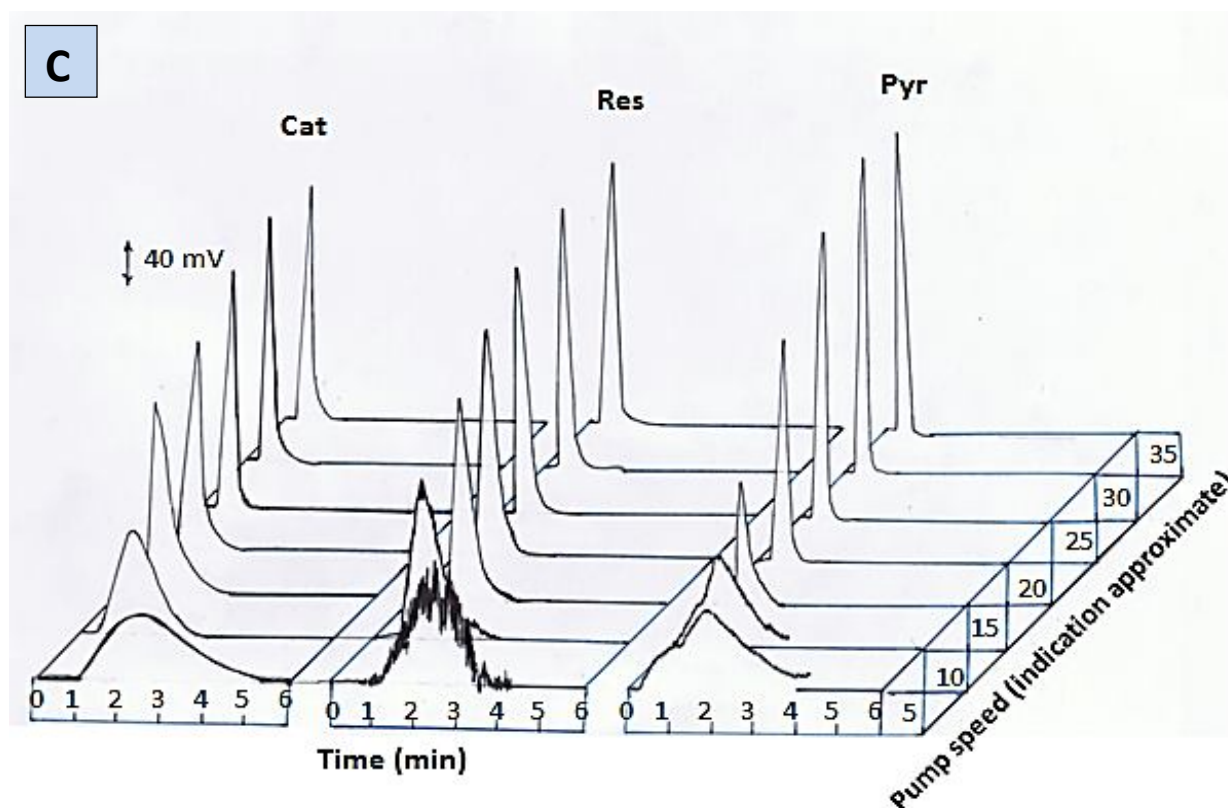


**Figure 6-** variation of flow rate on: A- transducer energy response for three org. comp., B- peak base width ( $\Delta t_b$ sec), and time for the departure of sample segment from injection valve reaching to the measuring flow Cell ( $t$  sec), C- response profiling using Ayah 3S<sub>BGR</sub>X 3-3D solar cell CFIA, for determination of Cat, Res, and Pyr.

**Sample volume:**

The study carried out using 2.1, and 2.4 ml.min<sup>-1</sup> as optimum flow rate for the carrier stream and Ce(IV) sulfate (40 mmol.L<sup>-1</sup> in acidic medium) respectively, with 20 mmol.L<sup>-1</sup> of Cat, Res, and Pyr. Variable sample volumes were used which equivalent to 110, 156, 165, 211, and 297  $\mu$ L which successively used with open valve mode. The results were tabulated in Table 4, which indicated that 165, 156, and 165  $\mu$ L were the optimum sample volume for the Cat, Res, and Pyr respectively, which gave sharp and smooth response profile, in addition to economy and decrease the analysis time. It was noticed that an increase in sample volume led to an increase in the height of response without effecting on the response profile up to the sample volume 165, 156, and 165  $\mu$ L for three organic compounds, more than led to a broadening at the peak maxima and an increase in the base width ( $\Delta t_b$ ) which was most probably attributed to continuous long time duration of color segment in front of the detector; this is illustrated in figure- 7 which shows these effects.

**Table 4-** Variation of injected sample volume on transducer energy response.

Type of analyte	Loop length (cm)	Sample volume ( $\mu\text{L}$ )	Average transducer energy response expressed as peak height $n=3, \bar{y}_i(\text{mV})$	RSD%	Confidence interval of the average response $\bar{y}_i \pm t_{0.05/2, n-1} \sigma_{n-1} / \sqrt{n}$	$\Delta t_b$ Sec
Cat	14.00	110	77.33	0.6	$77.33 \pm 1.15$	30
	19.82	156	104	0	$104 \pm 0$	36
	21.00	165	154	1.29	$154 \pm 4.97$	42
	26.80	211	226.67	1.01	$226.67 \pm 5.71$	48
	35.60	297	234.67	0.49	$234.67 \pm 2.85$	60
Res	14.00	110	182	1.09	$182 \pm 4.96$	18
	19.82	156	206	0.97	$206 \pm 2.40$	36
	21.00	165	212	0	$212 \pm 0$	38
	26.80	211	208	0	$208 \pm 0$	40
	35.60	297	202	0.99	$202 \pm 0.99$	42
Pyr	14.00	110	85.33	1.34	$85.33 \pm 2.85$	12
	19.82	156	112	1.1	$112 \pm 3.06$	15
	21.00	165	146	1.36	$146 \pm 4.97$	30
	26.80	211	162.67	1.41	$162.67 \pm 5.04$	36
	35.60	297	164.67	1.85	$164.67 \pm 7.57$	40

$\Delta t_b$  (sec): peak base width.

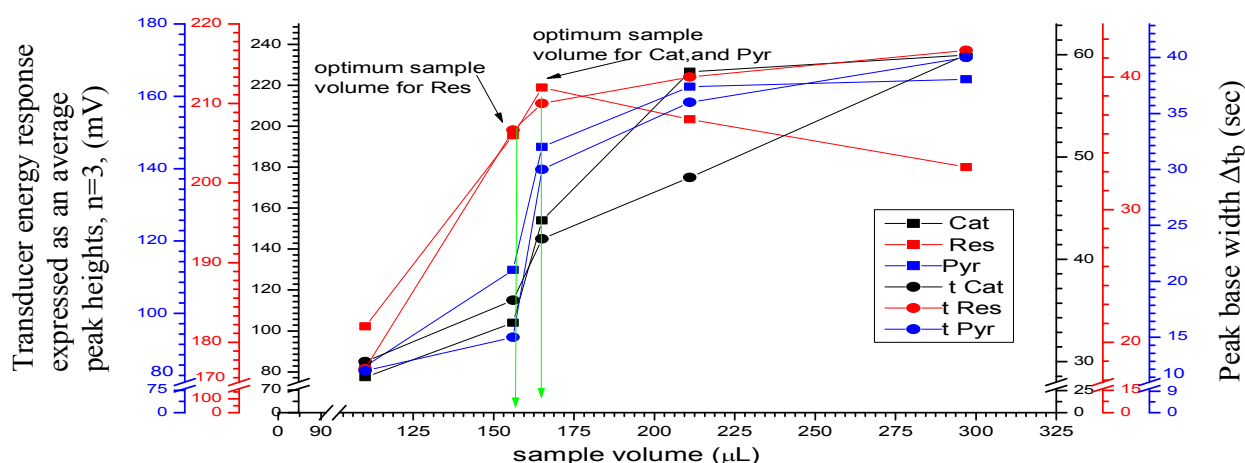


Figure 7- Variation of sample volume on transducer energy response, and peak base width ( $\Delta t_b$ ) for determination of Cat, Res, and Pyr.

**Purge time:**

Using different purge time for the sample segment i.e, the allowed time was 5-40 sec in addition to open valve mode for the three organic compounds sample to passing through the injection valve (injection mode) followed by turning the injection valve to the load position. Optimum sample volume of Cat, Res, and Pyr ( $30 \text{ mmol.L}^{-1}$ ) 165, 156, and 165  $\mu\text{L}$  respectively were used. Figure -8 shows the continuation of the increase in the height of response and  $\Delta t_b$  with increase of injection time up to open valve mode, therefore open valve mode as purge time was chosen as optimum time to the complete purge of sample segment from injection valve to the manifold of FIA system, which gave a better response profile (figure- 8B). The obtained results were tabulated in Table 5.

Table 5-Variation of purge time on the transducer energy response.

Type of analyte	Purge time (Sec)	Average transducer energy response expressed as peak height $n=3, \bar{y}_i$ (mV)	RSD%	Confidence interval of the average response $\bar{y}_i \pm t_{0.05/2, n-1} \sigma_{n-1} / \sqrt{n}$	$\Delta t_b$ (sec)
Cat	5	100	1.15	$100 \pm 2.85$	44
	10	110	0.9	$110 \pm 2.48$	46
	20	118	1.69	$118 \pm 4.97$	50
	30	120	0	$120 \pm 0$	54
	40	150	0	$150 \pm 0$	54
	Open valve	208	0.55	$208 \pm 2.85$	54
Res	5	140	1.4	$140 \pm 4.97$	24
	10	168	0	$168 \pm 0$	24
	20	209.33	0.55	$209.33 \pm 2.85$	28
	30	216	0	$216 \pm 0$	30
	40	220	0.9	$220 \pm 4.97$	34
	Open valve	230	0.86	$230 \pm 4.97$	36
Pyr	5	200	0.7	$200 \pm 3.48$	22
	10	285.33	0.8	$285.33 \pm 5.71$	24
	20	294	0.68	$294 \pm 4.97$	27
	30	298	0	$298 \pm 0$	30
	40	300	0.77	$300 \pm 5.71$	30
	Open valve	310	0.64	$310 \pm 4.97$	30

$\Delta t_b$  (sec): peak base width.

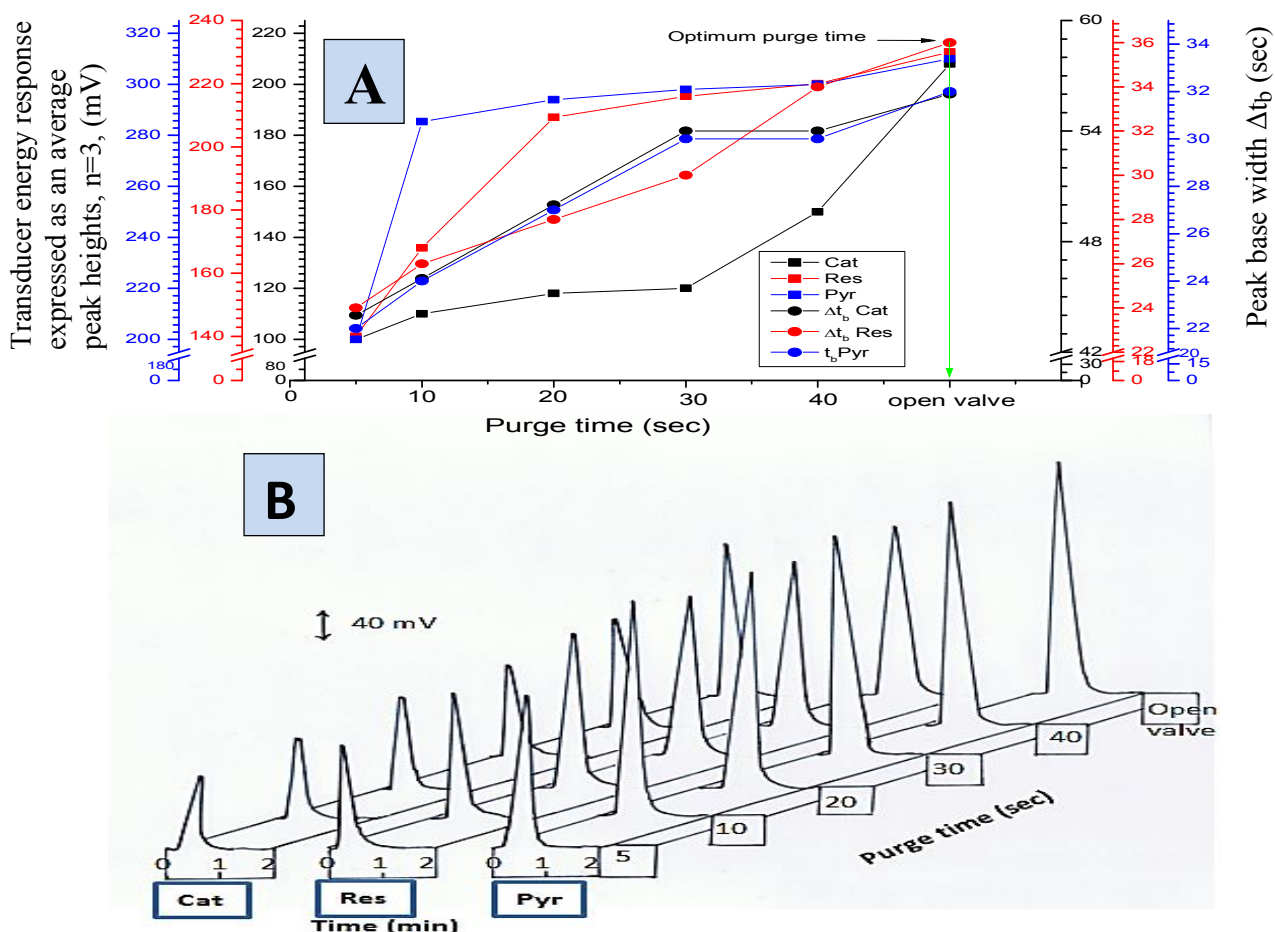


Figure 8- Variation of purge time on: A- transducer energy response, and peak base width ( $\Delta t_b$ ,sec). B-response profile using Ayah 3SBGRX 3-3D solar cellCFIA.

Incident light intensity:

Variable intensity of light source was used 0.6 – 1.3 volt for the green light emitted diode, and 0.6-1.2 for the blue light emitted diode by variation of light intensity channel in Ayah 3S<sub>BGR</sub> x 3- 3D solar cell CFIA microphotometer operation where read by AVO-meter. The optimum conditions were used; green light emitted diode (LED) 525 nm as an irradiation source for the Cat, and Res, while blue light emitted diode (LED) 470 nm as an irradiation source for the Pyr , 40 mmol.L<sup>-1</sup> of Ce(IV) sulfate, flow rate was 2.1, and 2.4 ml.min<sup>-1</sup> for the carrier stream and reagent line respectively, and sample volumes were 165, 156, and 165 μL of Cat, Res, and Pyr respectively (20 mmol.L<sup>-1</sup>). The obtained results tabulated in Table 6 which shows that an increase in the peak height with increase light intensity, therefore 1.2, and 0.9 volt was chosen as optimum voltage for the green light emitted diode(LED), and blue light emitted diode(LED) respectively, that can be supplied to give a better reproducible outcome as shown in figure- 9.

**Table 6** - Variation of incident light intensity on transducer energy response.

Type of Analyte	Intensity of Source (volt)	Average transducer energy response expressed as peak height n=3, $\bar{y}_i$ (mV)	RSD%	Confidence interval of the average response $\bar{y}_i \pm t_{0.05/2, n-1} \sigma_{n-1} / \sqrt{n}$
Cat	0.6	121.33	0.9	121.33 ± 2.85
	0.7	140	0	140 ± 0
	0.8	156	0	156 ± 0
	0.9	170	0.9	170 ± 3.8
	1.0	184	0	184 ± 0
	1.1	194	0	194 ± 0
	1.2	200	0.4	200 ± 1.99
	1.3	191.33	0.6	191.33 ± 2.85
Res	0.6	86	1.1	86 ± 2.33
	0.7	130	0.9	130 ± 3.4
	0.8	156.67	1.1	156.67 ± 4.27
	0.9	180.67	0.8	180.67 ± 3.57
	1.0	206	0	206 ± 0
	1.1	217.33	0.6	217.33 ± 3.22
	1.2	224	0	224 ± 0
	1.3	226	0.88	226 ± 4.97
Pyr	0.6	116	0.5	116 ± 1.44
	0.7	156	0.66	156 ± 2.53
	0.8	181.33	0.95	181.33 ± 4.27
	0.9	186	0.88	186 ± 4.04
	1.0	180	1.2	180 ± 5.36
	1.1	172	0	172 ± 0
	1.2	142.67	0.55	142.67 ± 1.93

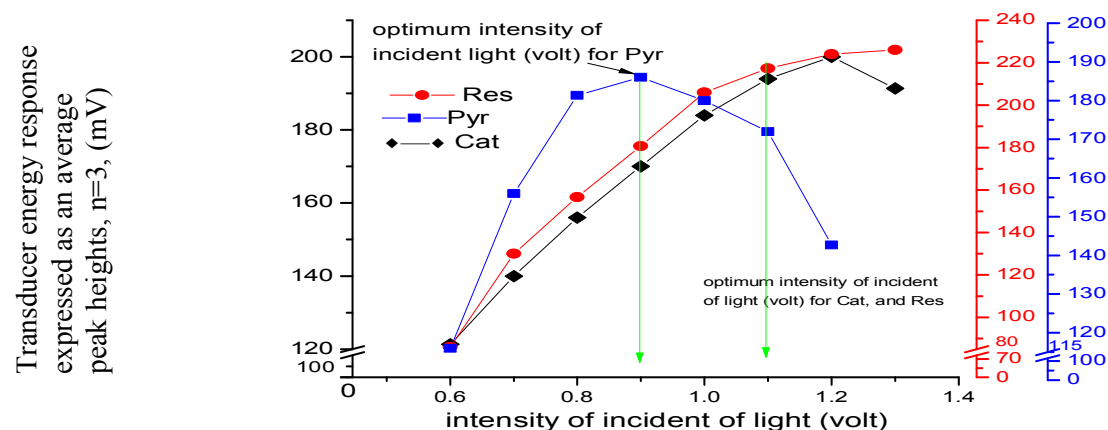


**Figure 9**- Variation of incident light intensity on transducer energy response .

**Calibration graph:**

At the established optimum conditions, a series of solution for three different organic compounds (1 - 100 mmol.L<sup>-1</sup>) were prepared. Each measurement was repeated three times. Transducer energy response of the average peak height ( mV ) was plotted against the concentration of threeorganic compounds A straight –line graph (figure-10) from 5 – 40 mmol.L<sup>-1</sup> of organic compounds were obtained. Above 40 mmol.L<sup>-1</sup> the value for correlation coefficient will decrease and deviate from linearity most probably due to the increase of the colored species in front of detector and due to the effect of inner filter of the high intensity colored species present in solution, which might be due to attenuation in transmitted light. The summaries of results were tabulated in Table 7.

**Table 7-** summary of calibration graph results for the determination of using org. comp. -Ce(IV) - H<sub>3</sub>O<sup>+</sup> system.

Type of analyte	Measured [x] mmol.L <sup>-1</sup>	Linear dynamic range mmol.L <sup>-1</sup> n = 11	$\hat{Y}_i$ (mV) = a ± ts <sub>a</sub> + b ± ts <sub>b</sub> [x] mmol.L <sup>-1</sup> at confidence level 95% , n - 2	r, r <sup>2</sup> %	t <sub>tab</sub>	$t_{cal} = t / \sqrt{\frac{n-2}{1-r^2}}$
Cat	1-100	5-40	-18.69±16.19+8.87±0.69[Cat]	0.9952 99.05%	2.306	<< 28.97
Res			70.11±8.39+ 5.86±0.34[Res]	0.9970 99.41%	2.306	<< 36.91
Pyr			-33.33±17.22+10.43±0.73[Pyr]	0.9960 99.22%	2.306	<< 32.03

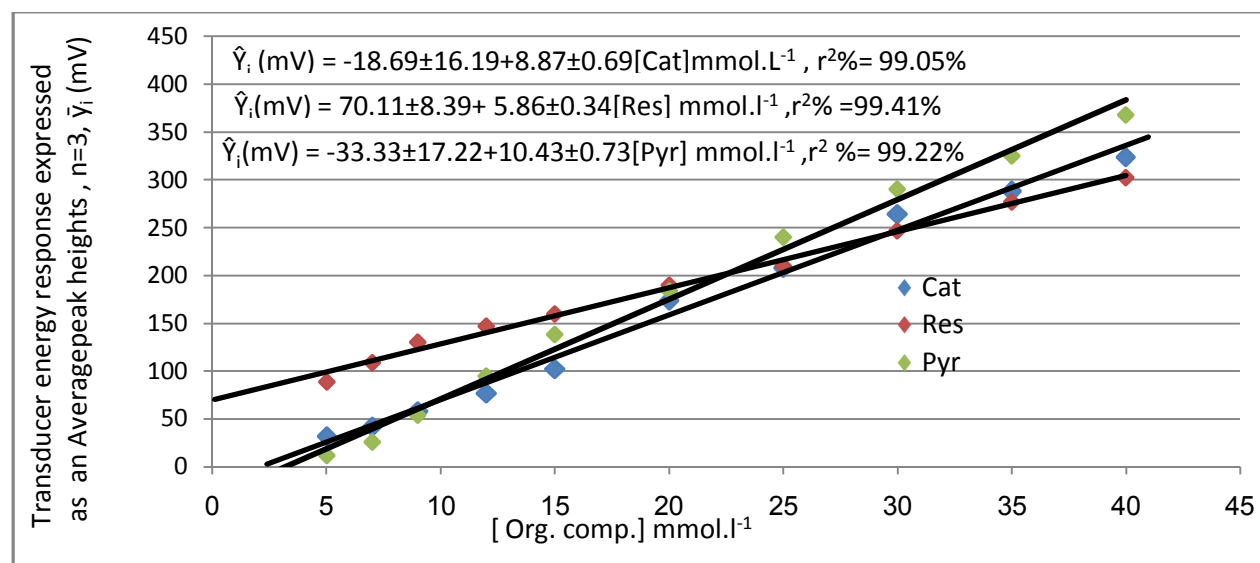


**Figure 10-** Calibration graph for the variation of Cat, Res, and Pyr concentration on transducer energy response expressed by linear equation using Ayah 3S<sub>BGRX3</sub>- 3D solar cell CFIAmicrphotometer.

**Limit of detection (L. O. D):**

Three different approaches were used for measuring L.O.D: gradual dilution of lowest concentration in the calibration graph, or detection based on the numerical value of slope or from the linear regression plot. Table 8 tabulated all these calculation value of detection limit for organic compounds with sample volume: 165,156, and 165µL respectively.

**Table 8**-Summary of limit of detection based on different approaches.

Type of analyte	Gradual dilution for minimum concentration	Based on the value of slope $X = 3S_B / \text{slope}$	Theoretical value from linear equation $\hat{Y}_i \text{ (mV)} = Y_B + 3S_B$
Cat	36.63 ng	61.45 ng	69.21 $\mu\text{g}$
Res	17.17 ng	87.96 ng	51.35 $\mu\text{g}$
Pyr	41.61 ng	59.85 ng	71.69 $\mu\text{g}$

$S_B$ : standard deviation of blank solution. ,  $X$ = value of L.O.D based on slope.

$Y_B$ : average response for the blank solution (equivalent to intercept in straight line equation).

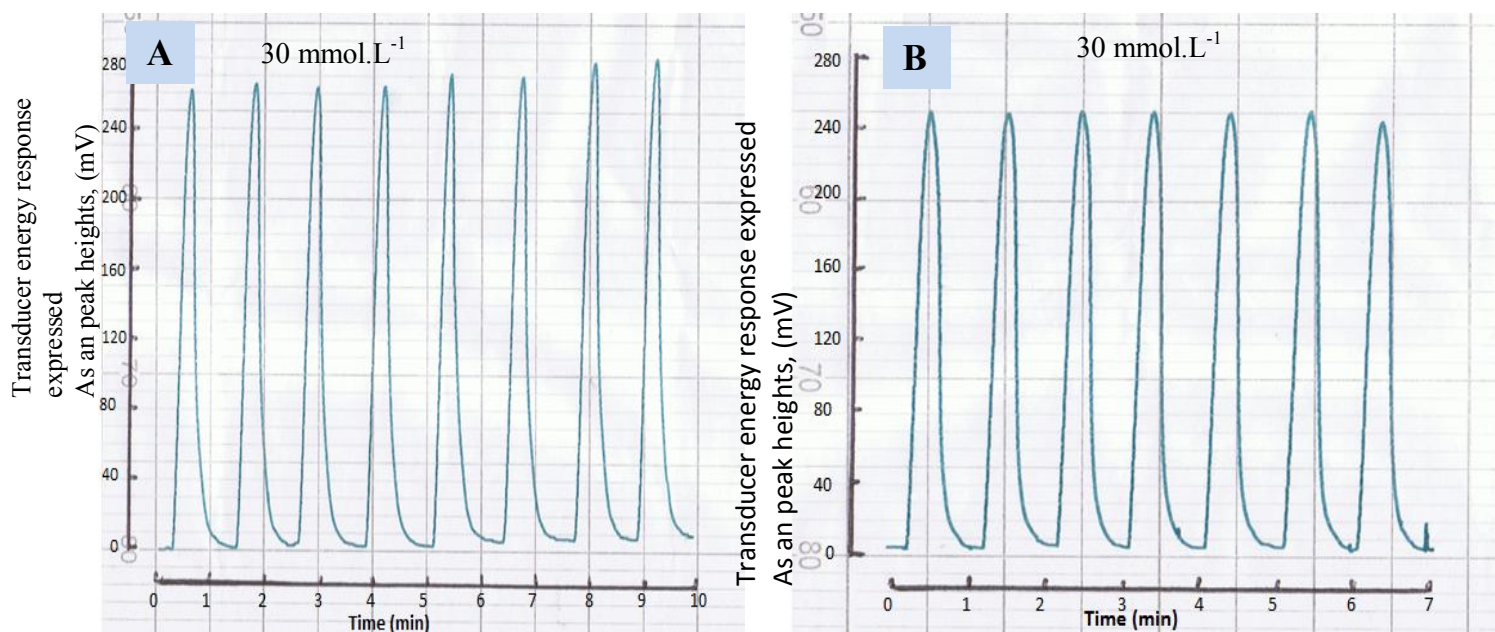
**Repeatability:**

The repeatability of measurement and the efficiency of homemade Ayah  $3S_{BGR} \times 3 - 3D$  solar cell CFIA microphotometer were studied at fixed concentrations of Cat, Res, and Pyr were used, mainly one concentration was used  $30 \text{ mmol.L}^{-1}$ , using the optimum parameters. The repeated measurements for eight and seven successive injections were measured and obtained results were tabulated in table 9 which shows that the percentage relative standard deviation was less than 1.4, 0.63, and 1.78 for Cat, Res, and Pyr respectively while figure-11 shows a kind of response-time profile for the used concentrations.

**Tablet 9** - Repeatability of Cat, Res, and Pyr results obtained for the formation of colored species.

Type of analyte	[x] $\text{mmol.L}^{-1}$	no. of injection	Average transducer energy response expressed as peak heights $\bar{y}_i \text{ (mV)}$	RSD %	Confidence interval of the average response 95 % confidence $\bar{y}_i \text{ (mV)} \pm t_{0.05/2, n-1} \sigma_{n-1} / \sqrt{n}$
Cat	30	8	268	1.4	$268 \pm 3.18$
Res	30	7	247.14	0.63	$247.14 \pm 1.57$
Pyr	30	8	290.25	1.78	$290.25 \pm 4.32$

[x] = Cat, or Res, or Pyr.



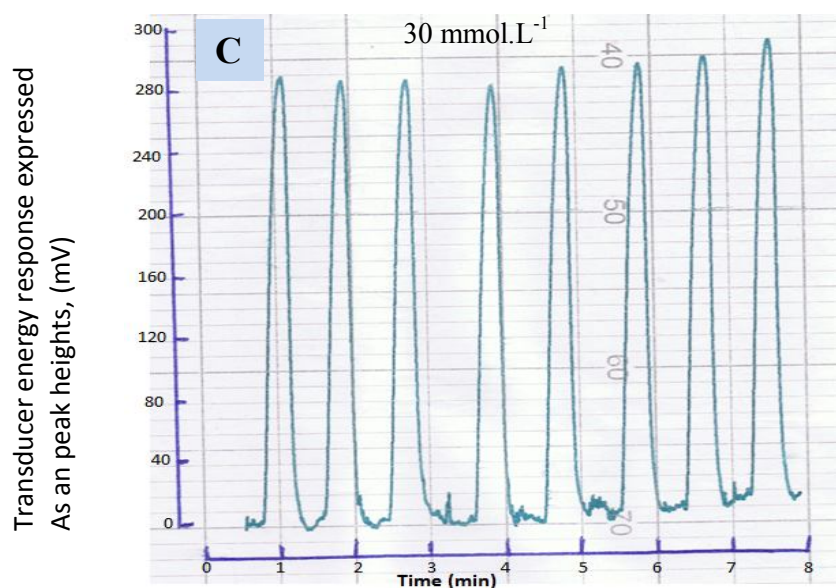


**Figure 11-** A Profile of successive repeatability measurements of: A-Cat, B- Res, C- Pyr (30 mmol.L<sup>-1</sup>) using Ayah 3S<sub>BGR</sub> x3S-3D solar cell CFIA microphotometer.

### Evaluation of the use of Ayah 3S<sub>BGR</sub> x 3S – 3D solar cell CFIA microphotometer in the determination of three organic compounds in pure commercial samples as an application:

The established method was used for the determination of Cat, Res, and Pyr, in pure formulation (pyrocatechol – Readeldehean- Germany, resorcinol- Randwin- india, and pyrogallol- Readeldehean- Germany), using Ayah 3S<sub>BGR</sub> x 3S – 3D solar cell CFIA microphotometer and was compared with classical spectrophotometric method via the measurement of  $\lambda_{max}$  at 492, 481, and 438 nm for Cat, Res, and Pyr respectively. The standard addition method was applied by prepared a series of solutions from each sample (Cat, Res, and Pyr) via transferring 0.25 mL, (500 mmol.L<sup>-1</sup>) of each sample, to five volumetric flask (25 mL), followed by the addition of ( 0 , 0.25 , 0.35 , 0.45 , and 0.75 ) from standard solution of Cat, Res, and Pyr (500 mmol.L<sup>-1</sup>) in order to have the concentration range from 0 – 15 mmol.L<sup>-1</sup>, for the preparation of standard additions calibration plot. The measurements were conducted by both methods.

Results were mathematically treated for standard additions method. The results were tabulated in Table 10 at confidence interval 95 %.

Paired t – test was used as shown in scheme 2. Which shows a comparison- treatment of data was subjected at two different paths.

First test: comparison between two methods of analysis (scheme 2-A), i.e. Ayah 3S<sub>BGR</sub> x 3S – 3D solar cell CFIA microphotometer [47] with UV-Vis spectrophotometric as shown in table 11-A.

Assumption:

(Null Hypothesis)  $H_0: \mu_{UV-vis} = \mu_{Ayah\ 3S_{BGR}\ x3-3D}$

Against (Alternative Hypothesis)  $H_1: \mu_{UV-vis} \neq \mu_{Ayah\ 3S_{BGR}\ x3-3D}$

From the results, it was noticed that two methods of analysis proved to indicate that there is no significant difference between the means of two different methods for analyzing three different organic compounds (Pyrocatechol, Resorcinol, and Pyrogallol).

Since calculated  $t_{value}$  of  $0.12 \ll 4.303$ , therefore,  $H_0$  is accepted against  $H_1$ .

now since  $H_0$  is valid.  $S_0$  a second test can be done on the basis that since  $H_0$  is valid and we have started at the same concentration (500 mmol.L<sup>-1</sup>), it mean that:

Method<sub>UV-vis</sub> = Method<sub>Ayah 3S<sub>BGR</sub> x3-3D</sub> (no difference for any method used).

And conc. of Pyrocatechol = conc. of Resorcinol = conc. of Pyrogallol (Equal concentration).



Therefore, we are going to use another second test to distinguish between the three different organic compounds, and does the three different compounds give the same product output. i. e. structural variation or effects regarded a not significant and they contribution the same effects therefore,

(Null Hypothesis)  $H_0 = \mu_{\text{Cat using both methods}} = \mu_{\text{Res using both methods}} = \mu_{\text{Pyr using both methods}}$

(Alternative Hypothesis)  $H_1 = \mu_{\text{Cat using both methods}} \neq \mu_{\text{Res using both methods}} \neq \mu_{\text{Pyr using both methods}}$

The values that were obtained for table 11-B, based on the scheme 2-B shows three pairs for comparison for pair 1: Cat. versus Res.

Assumption:

$H_0 = \mu_{\text{Cat}} = \mu_{\text{Res}}$  against  $H_1 = \mu_{\text{Cat}} \neq \mu_{\text{Res}}$

$t_{\text{calculate}} = |-0.81| \rightarrow t_{\text{Cal.}} = 0.81 \ll t_{\text{tab.}}(12.706)$ .

Therefore,  $H_0$  is accepted against  $H_1$  there is no significant difference in the contribution of both compounds (Cat and Res) to the reaction path.

Pair 2: Cat. Versus Pyr.

$H_0 = \mu_{\text{Cat}} = \mu_{\text{Pyr}}$  Against  $H_1 = \mu_{\text{Cat}} \neq \mu_{\text{Pyr}}$

$t_{\text{Calculated}} = 0.61 \ll t_{\text{tab}}(12.706)$

∴  $H_0$  is accepted against  $H_1$ .

i.e no significant difference in the contribution of both compounds (Cat and Pyr) to the reaction path.

Pair 3: Res versus Pyr.

$H_0 = \mu_{\text{Res}} = \mu_{\text{Pyr}}$  Against  $H_1 = \mu_{\text{Res}} \neq \mu_{\text{Pyr}}$

Since  $t_{\text{Calculated}} = 0.128 \ll t_{\text{tab}}(12.706)$ .

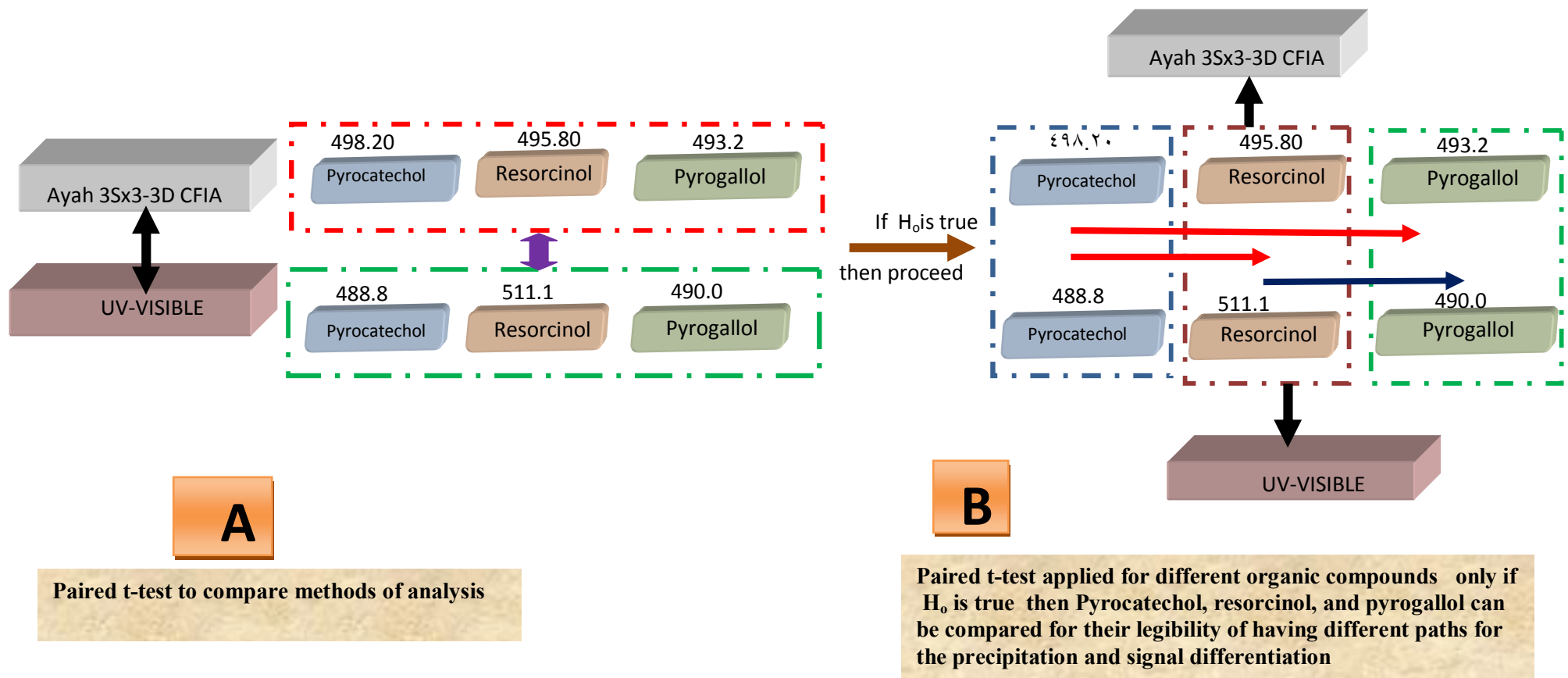
Therefore,  $H_0$  is accepted against  $H_1$ .

There is no significant difference using the two methods with the same concentration and structural effect does not add any significant difference. The above studied compounds give and behave similarly concerning used reaction and it cannot be differentiated or all what it concerns relating to the wags they are determined, therefore its have the same reaction pattern and cannot distinguish between them.

**Table 10**-Results for the determination of Cat, Res, and Pyr pure formulation using standard addition, with two methods Ayah 3S<sub>BGR</sub> X3 -3D solar cell CFIA microphotometer and UV-Vis spectrophotometric method.

analyte	Sample commercial name, company country.	Theoretical weight in 100 mL (g)	Theoretical concentration mmol.L <sup>-1</sup> , in 100 mL	Equation of standard addition curve at 95% for n-2 $\hat{Y}=a\pm s_a+t+b\pm s_b t[x]$	r r <sup>2</sup> %	Practical concentration mmol.L <sup>-1</sup> , in 25 mL	Practical concentration mmol.L <sup>-1</sup> , in 100 mL	Practical Weight(g) In 100 mL	Efficiency of determination (Rec %)
<b>UV - Vis spectrophotometer</b>									
Cat	Pyrocatechol, Readldehean, Germany.	5.505	500	27.95±6.01+5.61±0.67	0.9977 99.55%	4.982	498.2±6.89	5.485	99.64
				0.44±0.10+0.09±0.01	0.9954 99.09%	4.888	488.8±2.32	5.382	97.76
Res	Resoncinol, Randwin Indian	5.505	500	56.68±8.27+11.43±0.92	0.9989 99.79%	4.958	495.8±3.83	5.459	99.16
				0.46±0.09+0.09±0.01	0.9978 99.58%	5.111	511.1±7.31	5.627	102.22
Pyr	Pyrogallol, Readldehean, Germany.	6.3055	500	64.37±18.42+13.05±2.10	0.9960 99.22%	4.932	493.2±3.88	6.220	98.64
				0.49±0.09+0.10±0.10	0.9981 99.64%	4.900	490.0±3.32	6.179	97.99

$\hat{Y}_i$  = estimated value for energy transducer response (mV) or absorbance. X: [Cat], [Res], and [Pyr] mmol.L<sup>-1</sup>.



**Scheme 2: Paired t-test representation for the treatments of the data obtained in the analysis conducted by two different approaches. UV-Visible and Ayah3SX3-T-D-CFIA for three different organic compounds. (A) represent comparison of the two methods delivering data ; (B) represent IF  $H_0$  is accepted against the ALTERNATIVE  $H_1$  then the test is conducted to evaluate whether the structural effect of these three different organic compounds contribute to the reaction to the same extent .**

**Table 11-A:** paired t-test for two methods of analysis three organic compounds (Cat, Res, and Pyr, 500 mmol.L<sup>-1</sup>)

Pair	Practical concentration mmol.L <sup>-1</sup>			Mean $\bar{X}$ mmol.L <sup>-1</sup>	Xd mmol.L <sup>-1</sup>	$\bar{X}d$ mmol.L <sup>-1</sup>	$\sigma_{n-1}$	N	$t_{cal} = \frac{\bar{X}d \sqrt{n}}{\sigma_{n-1}}$	$t_{tab}$
	df									
Ayah 3S <sub>BGR</sub> x3 – 3D	498.2	495.8	493.2	495.73	9.4	-0.9	12.85	3	-0.12   << 4.303	
UV-Vis	488.8	511.1	490.0	496.63	-15.3			2		
					3.2					

Xd: differences between two methods,  $\bar{X}d$ : difference mean,  $\sigma_{n-1}$ : difference standard deviation, N: no. of organic compounds.

$t_{critical} = t_{tab} = t_{\alpha/2, n-1} = t_{0.05/2} = 4.303$ , df: degree of freedom

**Table 11-B:** paired t-test between three different organic compounds.

No. of pair	Paired differences		$t_{cal} = \frac{\bar{X}d \sqrt{n}}{\sigma_{n-1}}$	$t_{tab}$
	$\bar{X}d$ mmol.L <sup>-1</sup>	$\sigma_{n-1}$		
Pairs 1 Cat- Res	-9.95	17.46	-0.18   << 12.706	
Pairs 2 Cat- Pyr	1.9	4.38	0.61 << 12.706	
Pairs 3 Res- Pyr	11.85	13.08	1.28 << 12.706	

$t_{critical} = t_{\alpha/2, n-1} = t_{0.05/2}$ ,  $t = 1.706$ ,  $N = 2$ ,  $df = 1$ .

## Conclusion:

A spectrophotometric CFIA is proposed method for determination of Cat, Res, and Pyr with application in the quality control analysis. The method based on the oxidation of Cat or Res or Pyr by Ce(IV) sulfate in acidic medium forming brown product. The experimental point of view, the manipulation is very simple and sequential measurement was permitted with sample frequency up to 30 samples per hour. The proposed method uses cheaper instrument and reagent. In this paper a more effective faster determination was achieved by Ayah 3S<sub>BGR</sub> x 3-3D solar cell CFIA microphotometer, light emitted diode as source with a detection using solar cell. The standard additions method was used to avoid matrix effects and over high sensitivity without the need for heating or extraction. Also this method can be applied to micro determination of Cat, Res, and Pyr in pure formulation.

## Acknowledgement:

I would like to express my deepest gratitude to Prof. Dr. Issam M.A. Shakir Al-Hashimi for his appreciable advice, important comments, support and encouragement.

## Reference:

- Xu, F., 1996. Oxidation of phenols, anilines, and benzenethiols by fungal laccases: correlation between activity and redox potentials as well as halide inhibition. *Biochem.* 35, pp: 7608-7614.
- Miura, Y. Chiba, T. and Tomita, I. 2001. Tea catechins prevent the development of atherosclerosis in apoprotein E-deficient mice. *J. Nutr.*, 131, pp:27-32.
- Zhang, Y. G. M., Zeng, M. Tang, L. Huang, D. L. Jiang, X. Y. Chen, A. 2013. tyrosinase biosensor based on ordered mesoporous carbon-Au/L-lysine/Au nanoparticles for simultaneous determination of hydroquinone and catechol. *Analyst*, 138, pp: 3552-3560.
- Chen, C. Fangxin, H. Dehua, Y. Cun W. and Sun, C. 2012. Study on the application of reduced graphene oxide and multiwall carbon nanotubes hybrid materials for simultaneous determination of catechol, hydroquinone, p-cresol and nitrite. *Analytica Chimica Acta*, 724, pp: 40-46
- Klibanov, A.M. Alberti, B.N. Morris, E.D and Felshin, Z.M. 1980. Enzymatic removal of toxic phenols and anilines from wastewaters. *J. Appl. Biochem.* 2, pp: 414.

6. Yan, J. W. Jianping, J. Xiaoqiang, C. Qinggele and Zongding, H. **2006**. Mutation of *Candida tropicalis* by Irradiation with a He-Ne laser to increase its ability to degrade phenol. *Am. Soc. Microbiol.* pp: 226-231.
7. Weissermel, K. Arpe, H. J. **2003**. 4th Ed. "Benzene Derivatives" in *Industrial Organic Chemistry*. P: 366.
8. Maciel, R. Sant'Anna, G. M. Dezotti, J. **2004**. Phenol removal from high salinity effluents using Fenton's reagent and photo-Fenton reactions. *Chemosphere*, 57,(7) pp:711-719.
9. Jordan, W. Van Barneveld, H. Gerlich, O. Kleine, B. M. and Ullrich, J. **1985**. 5th Ed. "Phenol" in *Ullman's Encyclopedia of Industrial Chemistry*. Gerhards, VCH Verlagsgesellschaft, 19pp:3689-3707.
10. Hirakawa, K. Oikawa, S. Hiraku, Y. Hirokawa, I. and Kawanishi, S. **2002** Catechol and hydroquinone have different redox properties responsible for their differential DNA-damaging ability. *Chem. Res. Toxicol.* 15(1), pp:76-82.
11. Merck. **1989**. *The Merck Index*, 11th Ed. Rahway, NJ: Merck..
12. Milligan, P.W. and HaEgblom, M.M. **1998**. Biodegradation of resorcinol and catechol by denitrifying enrichment cultures. *Environ Toxicol Chem.* 17 pp: 1456-1461.
13. Neilson, A.H. Allard, A. S. and Hynning, P. A. **1991**. Distribution, fate and persistence of organochlorine compounds formed during production of bleached pulp. *Toxicol Environ Chem.* 30, pp: 3-41.
14. Capasso, R. Evidente, A. Schivo, L. Orru, G. Marcialis, M. and Cristinzio, G. **1995**. Antibacterial polyphenols from olive oil mill waste waters. *J. Appl. Bacteriol*, 79, pp: 393-398.
15. Panico, R. and Powell, W. H. **1994**. *A Guide to IUPAC Nomenclature of Organic Compounds*, Oxford: Blackwell Science.
16. Ullmann's. **2002**. *Ullmann's Encyclopedia of Industrial Chemistry*. 5th Ed. Gerhards, J. W. VCH Verlagsgesellschaft.
17. Kirk-Othmer. **1981**. *Hydroquinone, resorcinol, and catechol*. In: *Kirk-Othmer encyclopedia of chemical technology*, 3rd Ed. 13. New York, NY, John Wiley & Sons, pp. 39-69.
18. O'Neil, M. **2001**. Resorcinol. In: *The Merck index*, 13th Ed. Whitehouse Station, NJ, Merck, p. 1462.
19. Harris, J. **1990**. Rate of hydrolysis. In: Lyman WJ, Reehl WF. *Handbook of chemical property estimation methods*. 3 Ed. Washington, DC, American Chemical Society, pp. 7-48.
20. Sütfield, R. Petereit, F. Nahrstedt, A. **1996**. Resorcinol in exudates of *Nuphar lutea*. *Journal of Chemical Ecology*, 22 (12), pp: 2221-2231.
21. Yalkowsky, S.H. Dannenfelser, R. **1992**. *The aquasol database of aqueous solubility*, 5th Ed. Tucson, AZ, University of Arizona, College of Pharmacy .
22. Dressler, H. **1994**. *Resorcinol, its uses and derivatives*. 1st ED. New York, NY, Plenum Press.
23. Boer, J. Jemec, G. **2010**. Resorcinol peels as a possible self-treatment of painful nodules in hidradenitis suppurativa. *Clin Exp Dermatol*, 35 (1), pp: 36-40.
24. Cooksey, R. Gaitan, E. Lindsay, R. Hill, H. and Kelly, K. **1985**. Humic substances, a possible source of environmental goitrogens. *Organic Geochemistry*, 8 (1), pp:77-80.
25. Chou, C. Patrick, Z. **1976**. Identification and phytotoxic activity of compounds produced during decomposition of corn and rye residues in soil. *J. Chemical Ecology*, 2 (3), pp:369-387.
26. Budavari, S. **1996**. Pyrogallol. In: *The Merck Index*. 12<sup>th</sup> ed., Merck & Co., Inc., Whitehall, NJ. pp. 1375-1376.
27. Fiege, H. Voges, H. W. Hamamoto, T. Umemura, S. Iwata, T. Miki, H. Fujita, Y. Buysch, H. Garbe, D. and Paulus, W. **2000**. "Phenol Derivatives". *Ullmann's Encyclopedia of Industrial Chemistry*. Gerhards, J. W. VCH Verlagsgesellschaft.

28. Kumar, R. Gunasekaran, P. and Lakshmanan, M. **1999**. Biodegradation of tannic acid by *Citrobacter freundii* isolated from a tannery effluent. *J. Basic Microbiology*, 39, 161–168.
29. Abbaspour, A. and Baramakeh, L. **2005**. Simultaneous determination of antimony and bismuth by beta-correction spectrophotometry and an artificial neural network algorithm. *Talanta*. 65,(3), pp: 692-699.
30. Mazzei, J. da Silva, D. Oliveira, V. Hosomi, Z. do Val, R. Pestana, C. and Felzenszwalb, I. **2007**. Absence of mutagenicity of acid pyrogallol-containing hair gels. *Food and Chemical Toxicology*, 45, (4), pp: 643-648.
31. Clayton, G. D. and Clayton, F. **1981**. *Patty's Industrial Hygiene and Toxicology*, 3Ed., rev. Vol. IIA, John Wiley and Sons, New York. p. 2594.
32. O'donovan, L. and Brooker, J. **2001**. Effect of hydrolysable and condensed tannins on growth, morphology and metabolism *Streptococcus gallolyticus* (S. caprinus) and *Streptococcus bovis*. *Microbiology*, 147, pp:1025–1033.
33. Odenyo, R. Bishop, G. Asefa, R. Jamnadass, D. Odongo, P. and Osuji, O. **2001**. Characterization of tannin-tolerant bacterial isolates from East African ruminants. *Anaerobe*, 7, pp:5–15.
34. Cooper, R. and Wheatstone, K. **1973**. the determination of phenols in aqueous effluents. *Water Research*, 7, pp:1375–1384.
35. Shimizu, Y. Matsuto, S. Mizunuma, Y. and Okada, I. **1970**. Studies on the flavors of roast barley (mugi-cha). Part IV. Separation and identification of 5-hydroxymaltol, maltol, 5-methylcyclopent-2-en-2-ol-1-one and other compounds. *Agricultural and Biological Chemistry*, 34(6), pp:845–853.
36. Sooba, E. Tenno, T. Jáuregui, O. and Galceran, M. **1997**. Determination of phenols by liquid chromatography with electrochemical and UV detection. *Oil Shale*, 14(4), pp544–553.
37. Kahru, A. Põllumaa, L. Reiman, R. and Rätsep, A. **1999**. Predicting the toxicity of oil-shale industry wastewater by its phenolic composition. *Alternatives to Laboratory Animals*, 27, pp:359–366.
38. Kahru, A. Maloverjan, A. Sillak, H. and Põllumaa, L. **2002**. The toxicity and fate of phenolic pollutants in the contaminated soils associated with the oil-shale industry. *Environmental Science & Pollution Research International*, 1, 27–33.
39. Ghanem, M.A. **2007**. Electrocatalytic activity and simultaneous determination of catechol and hydroquinone at mesoporous platinum electrode, *Electrochem. Commun.* 9, pp: 2501–2506.
40. Carvalho, M. Mello, C. and Kubota, L. **2000**. Simultaneous determination of phenol isomers in binary mixtures by differential pulse voltammetry using carbon fibre electrode and neural network with pruning as a multivariate calibration tool. *Anal. Chim. Acta*, 420 pp:109–121.
41. Zhang, H. Q. **2005**. Simultaneous determination of hydroquinone and catechol at a glassy carbon electrode modified with multiwall carbon nanotubes. *Electroanalysis* 17, pp: 832–838.
42. Yu, J. Du, W. Zhao, F. and Zeng, B. **2009**. High sensitive simultaneous determination of catechol and hydroquinone at mesoporous carbon CMK-3 electrode in comparison with multi-walled carbon nanotubes and Vulcan XC-72 carbon electrodes, *Electrochim. Acta*. 54, pp: 984–988.
43. Zhao, D. Zhang, X. Feng, L.J. Jia, L. S. and Wang, S.F. **2009**. Simultaneous determination of hydroquinone and catechol at PASA/MWNTs composite film modified glassy carbon electrode, *Colloid Surf. B*. 74, pp: 317–321.
44. Nagaraja, P. Vasantha, R. Sunitha, and K. **2001**. A new sensitive and selective spectrophotometric method for the determination of catechol derivatives and its pharmaceutical preparations. *J. Pharm Biomed Anal*, 25(3-4), pp:417-24.
45. Afkhami, A. and Khatami, H. A. **2001**. Indirect Kinetic–Spectrophotometric Determination of Resorcinol, Catechol, and Hydroquinone. *J. Analytical Chemistry*, 56 ( 5), pp 429-432
46. Berenguer, V. N. **1975**. Spectrophotometric determination of catechol via the extraction of iron complexes with liquid ion exchangers Fresenius. *Zeitschrift für analytische Chemie*. 275 ( 2), p: 128.
47. Issam, M. A. S. and Nagam, S. T. **2012**. Ayah 3Sx3-3D solar cell FIA microphotometer, G01N29/00.

48. Jordan, W. Van barneveld, H. Gerlich, O. Kleine, M. and Ullrich, J., **1985**. "Phenol" in *Ullman's Encyclopedia of Industrial Chemistry*, 5th Ed. W. Gerhards, (Ed.), VCH Verlagsgesellschaft, A19 pp: 3689-3707.
49. Hudnall, P.M., **1985**. "Hydroquinone" in *Ullman's Encyclopedia of Industrial Chemistry*, 5<sup>th</sup> Ed. W. Gerhards, (Ed.), VCH Verlagsgesellschaft, A13 ,pp: 2941-2950.
50. Ehrfeld, W. Hessel, V. and Löwe. H. **2000**. "Electrochemical Microreactors" in *Microreactors: New Technology for Modern Chemistry*. Wiley-VCH, Weinheim, pp:166-169.
51. Nematollahi, D. Rafiee, M. and Fotouhi, L. **2009**. Mechanistic study of homogeneous reactions coupled with electrochemical oxidation of catechols. *J. Iran. Chem. Soc.*, 6 (3), pp: 448-476.
52. Sonali, S. Debarpita, G. and Jayanta, K. B. **2013**. Oxidation of Catechol using Titanium Silicate (TS-1) Catalyst: Modeling and Optimization. *Bulletin of Chemical Reaction Engineering and Catalysis*, 8 (2), pp: 167-177.